Rev Esp Cardiol. 2019;72(4):324–332

Original article

Digenic Heterozigosity in *SCN5A* and *CACNA1C* Explains the Variable Expressivity of the Long QT Phenotype in a Spanish Family

Paloma Nieto-Marín,[a,1] Juan Jiménez-Jáimez,[b,1] David Tinaquero,[a] Silvia Alfayate,[a] Raquel G. Utrilla,[a] María del Mar Rodríguez Vázquez del Rey,[c] Francesca Perin,[c] Geòrgia Sarquella-Brugada,[d] Lorenzo Monserrat,[e] Josep Brugada,[d] Luis Tercedor,[b] Juan Tamargo,[a] Eva Delpón,[a,2,*] and Ricardo Caballero[a,2]

[a] *Departamento de Farmacología, Facultad de Medicina, Universidad Complutense de Madrid, Instituto de Investigación Sanitaria Gregorio Marañón, CIBERCV, Madrid, Spain*
[b] *Unidad de Arritmias, Hospital Universitario Virgen de las Nieves, Instituto de Investigación Biosanitaria de Granada, Granada, Spain*
[c] *Departamento de Cardiología Pediátrica, Hospital Universitario Virgen de las Nieves, Granada, Spain*
[d] *Departamento de Cardiología Pediátrica, Hospital San Joan de Déu, Hospitalet de Llobregat, Barcelona, Spain*
[e] *Departamento de Cardiología, Health in Code, A Coruña, Spain*

Article history:
Received 21 November 2017
Accepted 6 March 2018

Keywords:
Long QT syndrome
CACNA1C
SCN5A
Cav1.2
Nav1.5
Patch-clamp
Channelopathies
I_{NaL}
I_{CaL}

ABSTRACT

Introduction and objectives: A known long QT syndrome-related mutation in Nav1.5 cardiac channels (p.R1644H) was found in 4 members of a Spanish family but only 1 of them showed prolongation of the QT interval. In the other 3 relatives, a novel missense mutation in Cav1.2 cardiac channels was found (p.S1961N). Here, we functionally analyzed p.S1961N Cav1.2 channels to elucidate whether this mutation regulates the expressivity of the long QT syndrome phenotype in this family.

Methods: L-type calcium current (I_{CaL}) recordings were performed by using the whole-cell patch-clamp technique in Chinese hamster ovary cells transiently transfected with native and/or p.S1961N Cav1.2 channels.

Results: Expression of p.S1961N channels significantly decreased I_{CaL} density. Using Ba as a charge carrier to suppress the Ca-dependent inactivation of Cav1.2 channels, we demonstrated that the mutation significantly accelerates the voltage-dependent inactivation of Cav1.2 channels decreasing the inactivation time constant. As a consequence, the total charge flowing through p.S1961N Cav1.2 channels significantly decreased. The effects of the p.S1961N Cav1.2 and p.R1644H Nav1.5 mutations alone or their combination on the action potential (AP) morphology were simulated using a validated model of the human ventricular AP. The p.S1961N Cav1.2 mutation shortens the AP duration and abrogates the prolongation induced by p.R1644H Nav1.5 channels.

Conclusions: The p.S1961N mutation in Cav1.2 channels decreased the I_{CaL}, an effect which might shorten ventricular AP. The presence of the loss-of-function Cav1.2 mutation could functionally compensate the prolonging effects produced by the Nav1.5 gain-of-function mutation.

La expresividad variable del síndrome de QT largo de una familia española se explica por la heterocigosis digénica en *SCN5A* y *CACNA1C*

Palabras clave:
Síndrome de QT largo
CACNA1C
SCN5A
Cav1.2
Nav1.5
Patch-clamp
Canalopatías
I_{NaL}
I_{CaL}

RESUMEN

Introducción y objetivos: En 4 miembros de una familia española se identificó una mutación en los canales cardiacos Nav1.5 (p.R1644H) descrita ya y relacionada con el síndrome de QT largo con anterioridad. Sin embargo, solo 1 de los portadores presentaba el intervalo QT prolongado. En los otros 3 individuos se identificó una nueva mutación con cambio de sentido en los canales cardiacos Cav1.2 (p.S1961N). En este trabajo se analizaron las características funcionales de los canales p.S1961N Cav1.2 para averiguar si dicha mutación regula la expresividad del síndrome de QT largo en esta familia.

Métodos: La corriente de calcio tipo L (I_{CaL}) se registró mediante la técnica de *patch-clamp* en células de ovario de hámster chino transfectadas transitoriamente con los canales cardiacos humanos en su forma nativa o mutada.

Resultados: La expresión de canales p.S1961N disminuye significativamente la densidad de la I_{CaL}. Al sustituir el ion calcio por bario para suprimir la inactivación dependiente del calcio de los canales Cav1.2, se demostró que la mutación acelera significativamente la inactivación dependiente del voltaje de los canales Cav1.2 y disminuye la constante de tiempo de inactivación. Como consecuencia, la carga total

* Corresponding author: Departamento de Farmacología, Facultad de Medicina, Universidad Complutense de Madrid, Plaza de Ramón y Cajal s/n, 28040 Madrid, Spain.
E-mail address: edelpon@med.ucm.es (E. Delpón).
[1] Both authors contributed equally to this work.
[2] Both authors are co-senior authors.

https://doi.org/10.1016/j.rec.2018.03.012
1885-5857/

que atraviesa los canales p.S1961N Cav1.2 disminuye significativamente. Los efectos que las mutaciones p.S1961N Cav1.2 y p.R1644H Nav1.5, por separado o en combinación, producen sobre las características de los potenciales de acción (PA) se simularon mediante un modelo matemático de PA ventriculares humanos. Los resultados demuestran que la mutación p.S1961N Cav1.2 abrevia la duración del PA y suprime la prolongación inducida por la mutación p.R1644H de los canales Nav1.5.

Conclusiones: La mutación p.S1961N en los canales Cav1.2 disminuye la I_{CaL}, un efecto que podría abreviar la duración de los PA ventriculares humanos. La presencia de esta mutación que disminuye la función de los canales Cav1.2 compensa funcionalmente los efectos producidos por la mutación de los canales Nav1.5 que aumenta su función y prolonga la duración de los PA.

Abbreviations

APD: action potential duration
I_{Ba}: current generated by Cav1.2 channels using Ba as a charge carrier
I_{CaL}: L-type Ca current
LQTS: long QT syndrome
VDI: voltage-dependent inactivation

INTRODUCTION

The long QT syndrome (LQTS) is an inherited primary arrhythmogenic syndrome characterized by a prolonged QT interval on the electrocardiogram (ECG) due to delayed ventricular repolarization and is associated with syncope, seizures, ventricular tachycardia (mainly *torsade de pointes*), and a high risk of sudden cardiac death.[1,2] Ventricular action potential (AP) duration (APD) is the result of a balance between depolarizing (Na and Ca) and repolarizing (K) currents. Thus, both an increase in the depolarizing or a decrease in the repolarizing currents could give rise to the different types of LQTS.[1,2]

LQTS type 3 is due to gain-of-function mutations in the *SCN5A* gene, which encodes the α-subunit of the sodium channels (Nav1.5) responsible for the cardiac sodium current (I_{Na}).[3] These mutations usually modify Nav1.5 channel kinetics by several biophysical mechanisms ultimately leading to an increase in the late component of the I_{Na} (I_{NaL}) that allows a persistent inward current during the plateau phase of the ventricular AP that lengthens the APD.[3]

CACNA1C, *CACNB2*, and *CACNA2D1* genes encode the pore forming α-subunit (Cav1.2) and the β2 and α2δ ancillary subunits, respectively, that form the cardiac Ca channel which generates the L-type Ca current (I_{CaL}).[4] Loss-of-function mutations in *CACNA1C* and *CACNB2* genes shorten the APD and have been associated with Brugada syndrome and short QT syndrome.[5,6] Conversely, gain-of-function mutations in the *CACNA1C* gene lead to prolongation of the ventricular APD and LQTS type 8.[7]

In this study, we identified a previously characterized gain-of-function mutation in *SCN5A* (encoding p.R1644H Nav1.5)[8] in 4 relatives of a Spanish family in which only 1 of the carriers had a LQTS type 3 phenotype. Genetic analysis of the other 3 relatives who had normal corrected QT (QTc) values demonstrated that they also carry a novel missense mutation in the *CACNA1C* gene encoding for p.S1961N Cav1.2 channels. Therefore, these family members harbour 2 variants in different genes (digenic heterozygosity). Thus, this study aimed to characterize the electrophysiological properties of p.S1961N Cav1.2 channels to elucidate whether the presence of this variant can ameliorate the APD prolongation and LQTS produced by the p.R1644H Nav1.5 mutant.

METHODS

Genetic Analysis

Clinical evaluation, including 12-lead ECG, of the family members was performed at the *Hospital Universitario Virgen de las Nieves* (Granada, Spain). The study was approved by the local ethics committee and conforms to the principles outlined in the Declaration of Helsinki. Each participant gave written informed consent.[9–11]

The whole codifying sequence and the flanking intronic regions of *KCNQ1, KCNH2, SCN5A, KCNJ2, KCNJ8, CACNA1C, AKAP9, KCNE1*, and *KCNE2* genes were sequenced using an Illumina 1500 Hiseq next-generation sequencing platform. Potentially pathogenic variants were confirmed using Sanger sequencing.[9–11] The pathogenicity of the variants was predicted according to the current recommendations of the American College of Medical Genetics and Genomics and the Association for Molecular Pathology (see details in the "Genetic analysis" section of the supplementary material).[12] Other exonic nonsynonymous variants found, not predicted as pathogenic, are described in the Table of the supplementary material.

Mutagenesis and Cell Transfection

The p.S1961N substitution in Cav1.2 (NP_000710.5) was introduced using the QuikChange Site-Directed Mutagenesis kit (Stratagene, United States) and confirmed by direct deoxyribonucleic acid (DNA) sequencing.[5,9,11,13] Chinese hamster ovary cells were transiently transfected with the cDNA encoding native (WT) or mutated Cav1.2 channels and the α2δ and β subunits (1:1.7:4 ratio).

Patch-clamping

Currents were recorded using the whole-cell patch-clamp configuration following previously described methods.[9,13] Uncompensated access resistance, cell capacitance, and peak I_{CaL} amplitude generated by WT Cav1.2 channels were 1.8 ± 0.4 MΩ, 16.2 ± 1.2 pF, and -521 ± 60 pA (n = 25), respectively. Therefore, no significant voltage errors (< 5 mV) due to series resistance were expected with the micropipettes used.

Mathematical Modelling of Ventricular Action Potential

To simulate the shapes of human ventricular AP, we employed the O'Hara-Rudy model previously validated and used for similar purposes.[14] The model was run at different driving frequencies (0.1-3 Hz) under baseline conditions (WT) or by incorporating the changes in I_{NaL} and I_{CaL} produced by p.R1644H Nav1.5 and p.S1961N Cav1.2 mutations, respectively.

Statistical Analysis

Results are expressed as mean ± standard error of the mean. Paired or unpaired *t* test or 1-way ANOVA followed by the Newman-Keuls test were used to assess statistical significance where appropriate. To take into account repeated sample assessments, data were analyzed with multilevel mixed-effects models. A value of $P < .05$ was considered statistically significant. An expanded Methods section is available in the supplementary material.

RESULTS

Case Description and Genetic Analysis

The proband (III.1) (arrow in Figure 1A) had a syncopal episode when he was 28 years old after a single dose of ciprofloxacin, a QT prolonging drug.[15] This suggested that he might have a genetic predisposition to drug-induced QT prolongation. Conversely, his clinical evaluation revealed a normal ECG with a Bazzett QTc of 420 ms (Figure 1B). However, both his mother (II.2) and grandmother (I.1), who had never experienced syncopal episodes, suddenly died at rest when they were 49 years old (clinical or genetic data were not available). Therefore, his family history of sudden cardiac death encouraged the evaluation of the proband's relatives. The proband's sister (III.2) showed an inferior atrial rhythm at 60 beats per minute, normal PR and QRS durations, and a slightly widened T wave (Figure 1A,1B). However, her QT properly shortened during exercise and the QTc was also normal (430 ms). One of the proband's nephews (IV.1), a 13-year-old boy, had an ECG with a late T wave after a long flat ST-segment, which resulted in a markedly prolonged QTc (558 ms) (Figure 1B). Conversely, IV.2 showed a QTc of 420 ms with normal T wave (Figure 1B). The rest of the relatives studied (white symbols in Figure 1A) have been and are currently asymptomatic, with completely normal ECGs.

Considering the clinical data, a genetic analysis by means of next-generation sequencing (see Methods) was offered to both the proband, who initially refused it, and his sister, who accepted. Genotyping of the proband's sister identified 2 mutations (digenic heterozigosity). These mutations were thereafter sequenced, using the Sanger method, in the proband (who finally accepted) and the rest of the relatives studied. The first mutation, predicted as pathogenic (see the "Genetic analysis" section of the supplementary material), appeared in *SCN5A* (NC_000003.11:g.38592932C>T according to GRCh37) leading to the arginine-to-histidine substitution of the residue 1644 (p.R1644H) in Nav1.5 channels. This mutation was previously described in several families with LQTS type 3 and has never been related to any other arrhythmic phenotype, including the Brugada syndrome.[8,16–18] Functional studies revealed that the p.R1644H mutation produces a marked increase in I_{NaL} (gain-of-function), which explains the APD and QT prolongation.[8,16] The p.R1644H Nav1.5 mutation was also found in the proband and nephews, but not in any other of the relatives tested (Figure 1A). In the proband's sister, the proband, and 1 of his nephews (Figure 1A) a mutation in the *CACNA1C* gene was also identified (NC_000012.11:g.2797710G>A) (Figure 2B) that leads to a serine-to-asparagine substitution in the Cav1.2 channel at position 1961 (p.S1961N) (Figure 2A). The serine residue is highly preserved at the equivalent position among different species (Figure 2C) and the mutation has not been annotated previously in any public database. Importantly, the p.S1961N Cav1.2 mutation is also carried by II.4 and III.4 but both individuals had normal ECGs and have never experienced any arrhythmic event.

Therefore, family members who showed digenic heterozygosity do not exhibit LQTS type 3 phenotype, while IV.1, who is the only one who carries only the *SCN5A* mutation, does. Thus, we decided

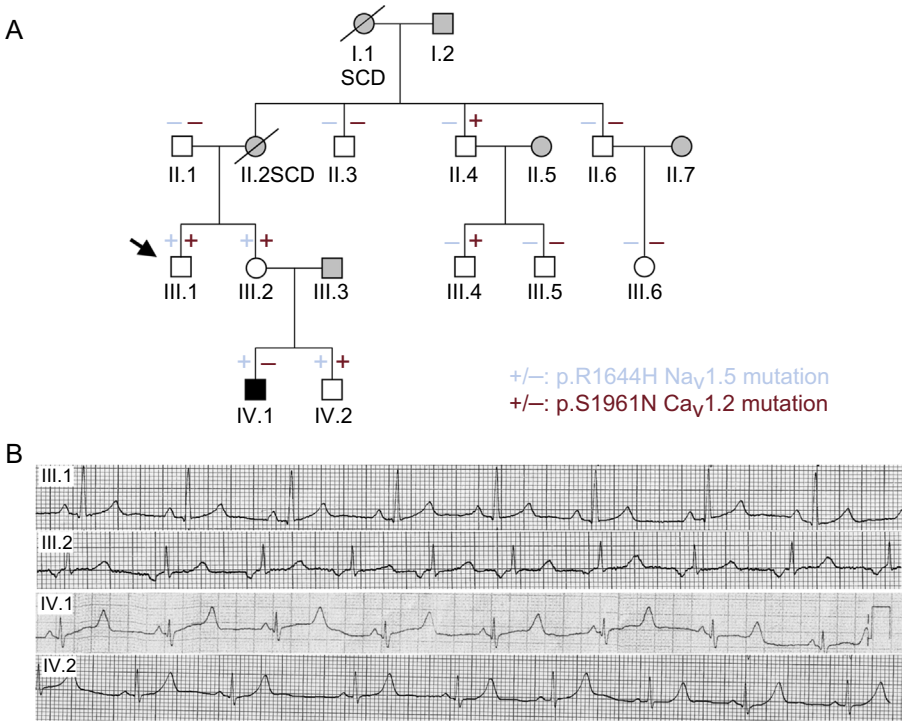

Figure 1. A: pedigree of the family (females [○] and males [□]). The arrow indicates the proband. Diagonal lines indicate deceased patients. + and – indicate individuals with and without the p.R1644H Nav1.5 (blue) and p.S1961N Cav1.2 (red) variants, respectively. Black symbols indicate long QT syndrome-affected individuals, while grey symbols depict individuals without genetic testing. White symbols represent studied individuals not affected by any clinical phenotype. B: electrocardiogram of III.1, III.2, IV.1, and IV.2. SCD, sudden cardiac death.

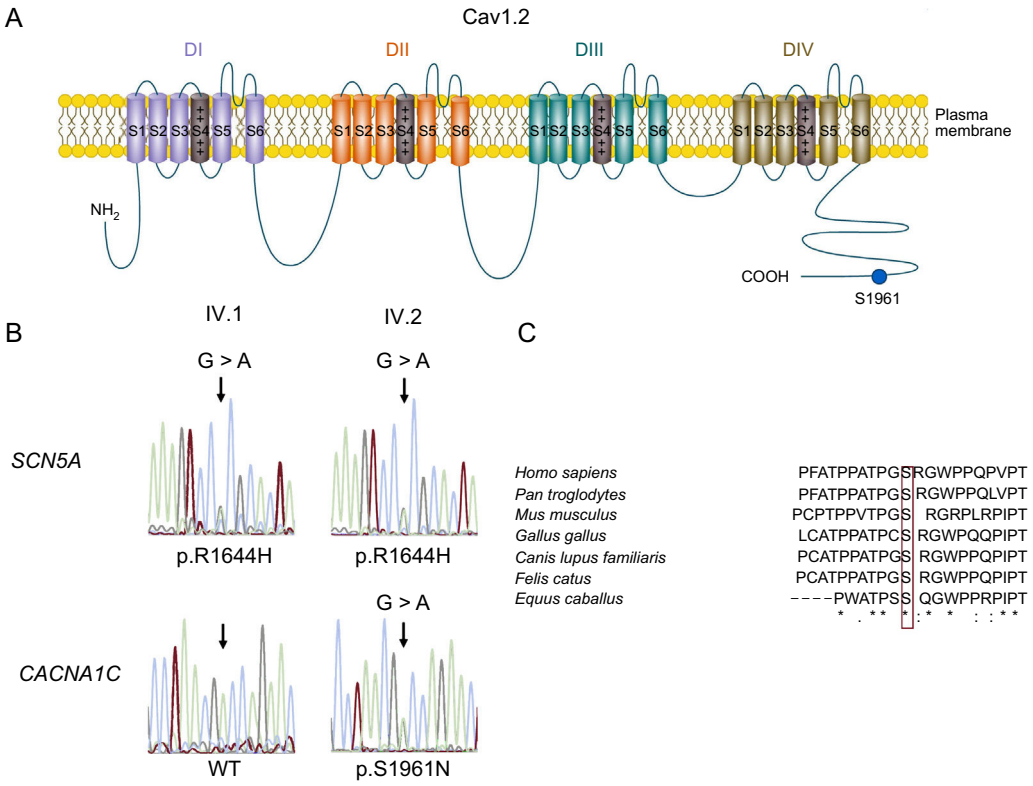

Figure 2. A: scheme of the L-type cardiac calcium channel. B: DNA sequence chromatograms of IV.1 and IV.2 depicting the heterozygous variation (NC_000003.11:g.38592932C>T) of the *SCN5A* gene leading to the missense mutation p.R1644H in both individuals (top) and a WT sequence (left) and the heterozygous mutation (NC_000012.11:g.2797710G>A) (right) of the *CACNA1C* gene, which results in the p.S1961N missense mutation (bottom). C: sequence alignment of the regions surrounding S1961 residue in Cav1.2 channels in several species. The box highlights the conservation of this residue. "*" identical residues. ":" and "." indicate conservation between groups of strongly and weakly similar properties, respectively. DNA, deoxyribonucleic acid; WT, native form of the channel.

to functionally characterize the p.S1961N Cav1.2 mutation to elucidate whether the presence of this variant can ameliorate the APD prolongation and LQTS type 3 produced by the p.R1644H Nav1.5 mutant.

Functional Characterization of p.S1961N Cav1.2 Channels

Figure 3A shows I_{CaL} traces recorded at potentials between -50 and +70 mV in Chinese hamster ovary cells expressing human cardiac WT or p.S1961N Cav1.2 channels along with the α2δ and β subunits. Peak density of the currents generated by p.S1961N Cav1.2 channels (-26.4 ± 1.4 pA/pF; $P < .05$) was approximately 25% lower than that generated by WT channels (-35.5 ± 3.0 pA/pF) (Figure 3A, 3B). In another group of experiments, cells were cotransfected (0.5:0.5 ratio) with the cDNA encoding WT and p.S1961N Cav1.2 channels considering the heterozygous condition of the mutation carriers. Under these conditions, peak current density was not statistically different to that generated by WT and p.S1961N channels separately (Figure 3B; $P > .05$). Figure 3C shows the voltage dependence of the activation of WT, p.S1961N, and WT+p.S1961N Cav1.2 channels obtained by plotting the normalized conductance (estimated by using equation #1; see section patch-clamping of the supplementary material) as a function of the membrane potential. The fit of a Boltzmann function to the data, yielded the midpoint (V_h) and the slope (k) of the curves, which almost overlap (Figure 3C). Thus, V_h and k values of the 3 curves were not significantly different (Table). The fit of the equation #2 (see section patch-clamping of the supplementary material) to the current density-voltage data in each experiment yielded the E_{rev} which averaged 74.9 ± 2.7 mV for WT channels. The mutation, either expressed alone or in combination with WT channels, did not modify the E_{rev} ($P > .05$) (Table).

Figure 4A shows superimposed I_{CaL} traces elicited when applying 500 ms-pulses from -80 to +20 mV in cells expressing WT or p.S1961N Cav1.2 channels (currents generated by WT+p.S1961N channels were omitted for clarity). Activation kinetics of Cav1.2 channels was not modified by the p.S1961N mutation alone or cotransfected with WT channels (Table; $P > .05$). Conversely, the mutation significantly accelerated the time course of current inactivation (Figure 4A), decreasing the fast time constant of inactivation (τ_{fast}) calculated by the biexponential fit to the current decline (Figure 4B and Table). Interestingly, τ_{fast} of the current generated by WT+p.S1961N channels was intermediate (Figure 4B and Table). Therefore, to accurately analyze the effects produced by the p.S1961N mutation on the total Ca influx we measured the charge density generated by WT, p.S1961N, and WT+p.S1961N Cav1.2 channels at each membrane potential (Figure 4C). The density was calculated by normalizing the charge crossing the membrane, estimated from the integral of current traces, to the cell capacitance (methods of the supplementary material). Due to the combined effects of the mutation on the peak current density and on the inactivation kinetics, the charge was significantly reduced by the p.S1961N mutation either alone or together with WT (Figure 4C).

Figure 4D (top) shows I_{CaL} traces generated by WT Cav1.2 channels with the protocol used to assess the voltage dependence of inactivation and construct the inactivation curves (methods of the supplementary material) (Figure 4D bottom). Neither the V_h

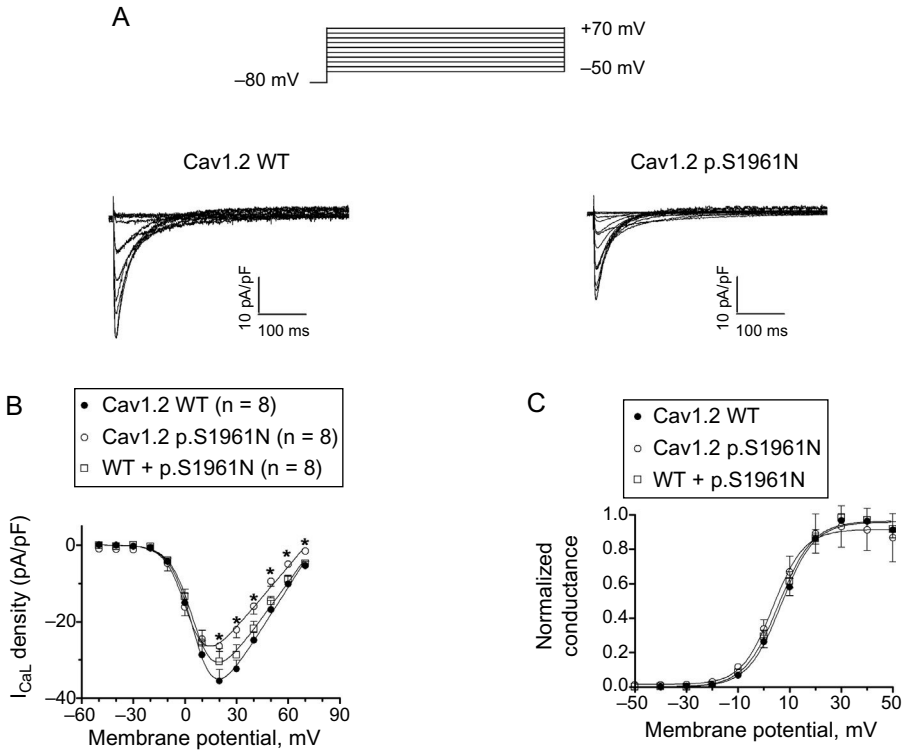

Figure 3. A: currents generated by WT or p.S1961N Cav1.2 channels. B,C: mean density-voltage (B) and conductance-voltage curves (C) for I_{CaL} generated by WT, p.S1961N or WT+p.S1961N Cav1.2 channels. Each point represents the mean ± standard error of the mean of (n) experiments. In B, $^{*}P < .05$ vs Cav1.2 WT. I_{CaL}, L-type Ca current. WT, native form of the channel.

nor the *k* of the inactivation curves were modified by the p.S1961N mutation either alone or in combination with WT channels (Figure 4D and Table).

The p.S1961N Mutation Accelerated the Cav1.2 Voltage-dependent Inactivation

Inactivation of Cav1.2 channels consists of 2 independent mechanisms, the Ca-dependent (CDI) and the voltage-dependent inactivation (VDI). We tested the effects of p.S1961N mutation on the VDI by using Ba as charge carrier since Ba currents (I_{Ba}) do not exhibit CDI.[19] Figure 5A shows I_{Ba} traces generated in 2 Chinese hamster ovary cells transfected with WT or p.S1961N Cav1.2 channels, respectively. Inactivation decay of I_{Ba} defined by a monoexponential function was markedly accelerated by the mutation (Figure 5B and Table). Furthermore, the mutation significantly decreased the peak I_{Ba} and Ba charge densities, the decrease in the charge being greater than that of the peak current (Figure 5C and Figure 5D). Finally, the voltage dependence of I_{Ba} inactivation was not modified by the mutation (Figure 5E and Table). All these results strongly suggested that p.S1961N mutation accelerates the VDI of Cav1.2 channels.

Simulation of the Effects of p.S1961N Mutation on the Cardiac Action Potential

The effects of the p.S1961N Cav1.2 and p.R1644H Nav1.5 mutations, alone or combined, on the AP characteristics were simulated using a validated model of human endocardial ventricular myocytes (Figure 6).[14] The model was run in baseline conditions (WT) or by introducing the kinetic and conductance changes produced by the p.S1961N Cav1.2 mutation. To simulate

Table
Biophysical Properties of WT and Mutant Cav1.2 Channels

			Activation			Inactivation			
Cav1.2 construct (I_{CaL})	*Charge at +20 mV (pC/pF)*	*E_{rev} (mV)*	*V_h (mV)*	*k*	*τ (ms)*	*V_h (mV)*	*k*	*τ_{fast} (ms)*	*τ_{slow} (ms)*
WT (n = 8)	-1.7 ± 0.2	74.9 ± 2.7	7.3 ± 1.4	6.4 ± 0.3	1.2 ± 0.03	-19.1 ± 1.2	7.0 ± 0.9	22.4 ± 0.3	89.4 ± 5.1
p.S1961N (n = 8)	-1.0 ± 0.1[a]	73.2 ± 1.3	5.5 ± 1.3	6.8 ± 0.2	1.1 ± 0.1	-20.6 ± 2.2	7.8 ± 0.5	14.7 ± 1.1[a]	78.3 ± 6.0
WT+p.S1961N (n = 9)	-1.4 ± 0.1[a,b]	76.1 ± 0.9	6.1 ± 1.6	6.9 ± 0.2	1.2 ± 0.1	-21.1 ± 2.3	7.9 ± 0.6	18.1 ± 1.0[a,b]	90.3 ± 3.9
Cav1.2 construct (I_{Ba})	*Charge at +10 mV (pC/pF)*	*E_{rev} (mV)*	*V_h (mV)*	*k*	*τ (ms)*	*V_h (mV)*	*k*	*τ (ms)*	
WT (n = 13)	-4.5 ± 1.1	55.7 ± 0.9	-3.4 ± 1.3	4.9 ± 0.4	1.8 ± 0.1	-27.9 ± 4.4	8.7 ± 1.6	67.5 ± 3.3	
p.S1961N (n = 10)	-1.6 ± 0.3[a]	54.8 ± 1.7	-0.8 ± 1.3	5.1 ± 0.3	1.5 ± 0.2	-30.0 ± 4.6	7.9 ± 1.0	43.1 ± 3.9[a]	

E_{rev}, reversal potential; I_{Ba}, current generated using Ba as a charge carrier; I_{CaL}: L-type Ca current; τ, time constants of activation (I_{CaL})/inactivation (I_{Ba}) obtained by fitting a monoexponential function to the current traces recorded at +20 mV. τ_{fast} and τ_{slow}, fast and slow time constants of inactivation (I_{CaL}) obtained by fitting a biexponential function to the current traces recorded at +20 mV; V_h and *k*, midpoint and slope values of the activation and inactivation curves; WT, native form of the channels. Values are the mean ± standard error of the mean of (n) experiments in each group.

[a] $P < .05$ vs WT.

[b] $P < .05$ vs p.S1961N.

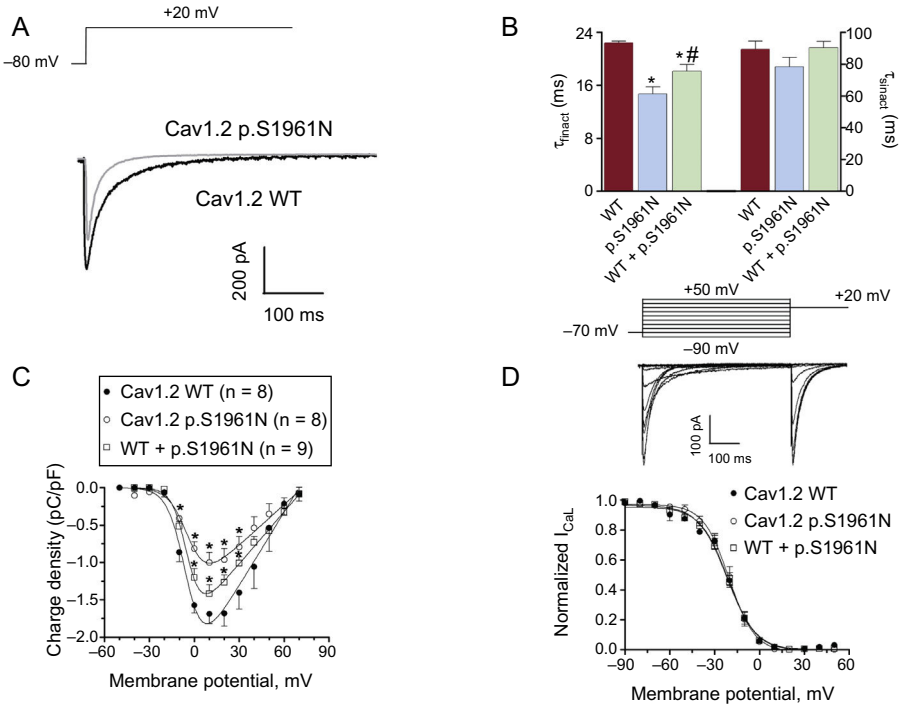

Figure 4. A: superimposed current traces generated at +20 mV by WT or p.S1961N Cav1.2 channels. B: fast and slow time constants of inactivation obtained at +20 mV in cells expressing WT, p.S1961N or WT+p.S1961N Cav1.2 channels. C: charge estimated as the integral of the current traces recorded as a function of the membrane potential in the 3 groups. D: Top: currents generated by WT Cav1.2 channels using the protocol shown. Bottom: inactivation curves for WT, p.S1961N or WT+p.S1961N Cav1.2 channels. Each bar/point represents the mean ± standard error of the mean of ≥ 8 experiments. *$P < .05$ vs Cav1.2 WT. WT, native form of the channel.

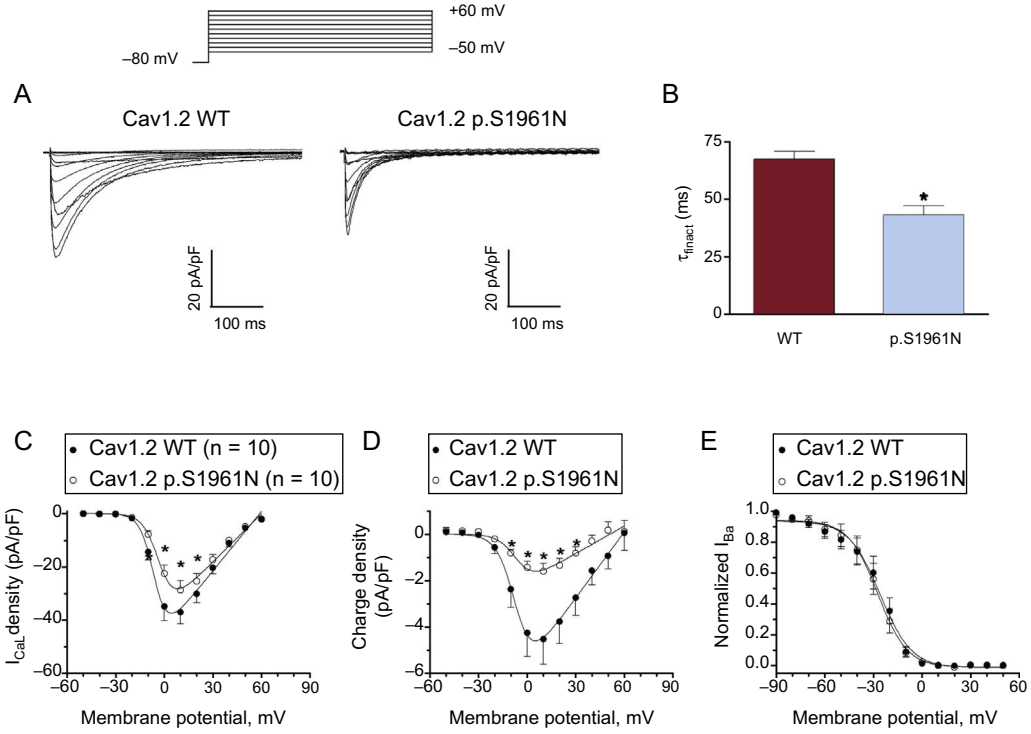

Figure 5. A: I_{Ba} traces generated by WT or p.S1961N Cav1.2 channels. B-E: inactivation time constants obtained at +10 mV (B), mean current density- (C), charge-density voltage (D), and inactivation (E) curves for I_{Ba} generated by WT or p.S1961N Cav1.2 channels. Each point represents the mean ± standard error of the mean of 10 experiments. In B-D, *$P < .05$ vs Cav1.2 WT. WT, native form of the channel.

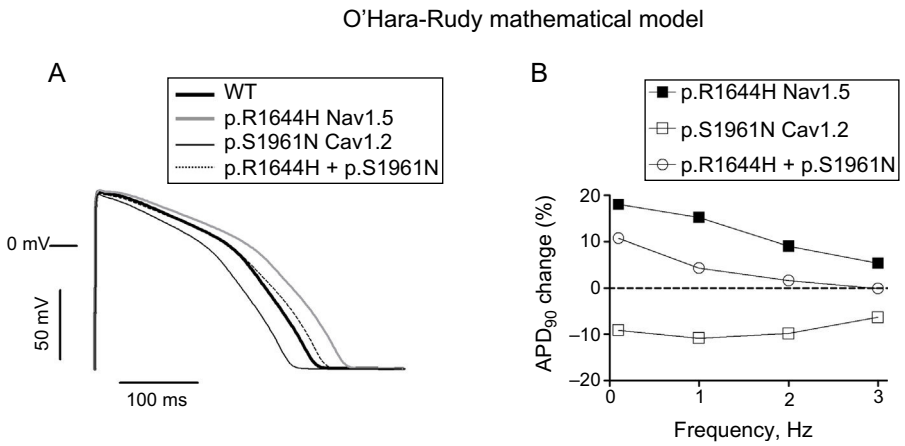

Figure 6. A: action potential traces generated by the O'Hara-Rudy model in endocardial ventricular myocytes at 1 Hz in baseline conditions (WT), or in the presence of the p.R1644H Nav1.5 and p.S1961N Cav1.2 mutations alone or in combination. B: percentage of APD_{90} prolongation (positive values) or shortening (negative values) induced by each mutation alone or in combination in endocardial cells driven at 0.1-3 Hz. APD, action potential duration; WT, native form of the channel.

the effects of the p.R1644H mutation the I_{NaL} conductance was increased ≈3-fold, as previously described.[8] Figure 6A shows the simulated AP traces obtained at 1 Hz. p.R1644H Nav1.5 lengthened the APD_{20}, APD_{50}, and APD_{90} by 17.4%, 17.1%, and 15.2%, respectively. Due to the I_{CaL} reduction, p.S1961N Cav1.2 shortened APD_{20}, APD_{50}, and APD_{90} by 21.7%, 14.3%, and 10.8%, respectively (Figure 6A). Interestingly, the AP traces corresponding to p.R1644H+p.S1961N and WT were almost undistinguishable, and only a small prolongation of the APD_{90} (4.3%) was observed. Figure 6B depicts the APD_{90} change (prolongation or shortening) induced by each mutation in cells driven at different frequencies (0.1-3 Hz). Prolongation induced by p.R1644H Nav1.5 was maximum at low frequencies and decreased progressively at faster rates. The shortening induced by p.S1961N Cav1.2 was similar at frequencies between 0.1 and 2 Hz (≈10%), decreasing slightly at 3 Hz. In the presence of p.S1961N, the prolongation induced by p.R1644H was reduced, being completely suppressed at high frequencies (2 and 3 Hz).

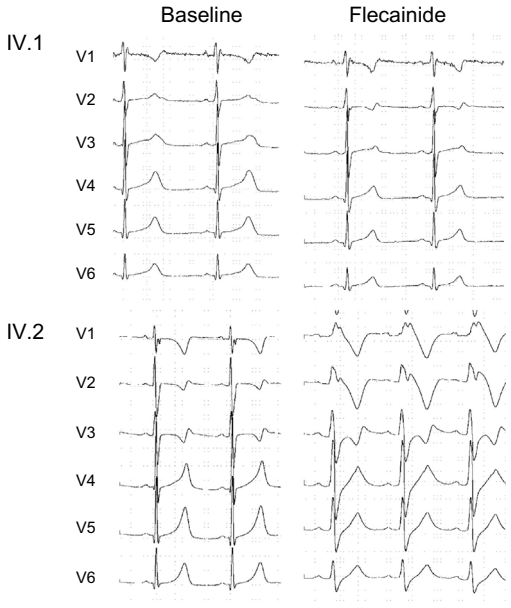

Figure 7. Electrocardiogram recordings (V_1-V_6) of IV.1 (top) and IV.2 (bottom) before (baseline) and after 10 minutes of intravenous infusion of flecainide at 2 mg/kg.

Therapeutic Implications of the Functional Results

Expert consensus recommendations on LQTS therapeutic interventions consider that I_{NaL} inhibitors, such as flecainide, can be useful as add-on therapy for the treatment of LQTS type 3 patients.[20] Accordingly, we tested the safety and efficacy of flecainide by infusing the drug (2 mg/kg) under a controlled situation, before the implementation of a treatment of the IV.1 patient with this drug. Figure 7A shows that in the gain-of-function *SCN5A* mutant carrier, flecainide shortened the QT interval (QTc decreased from 558 to 470 ms) without inducing any arrhythmic response. Therefore, in this child, oral flecainide was added-on the maximal tolerated dose of atenolol (50 mg od) for arrhythmic event prophylaxis.

Conversely, loss-of-function *CACNA1C* mutations have been related to Brugada syndrome[5] which is definitively diagnosed when a type I ST-segment elevation in precordial leads is observed after intravenous administration of flecainide. Since our functional analysis demonstrated that the p.S1961N Cav1.2 mutation reduces the I_{CaL} density, we wondered whether the presence of the *CACNA1C* mutation would lead to a Brugada syndrome-like pattern in the presence of flecainide.[11] Therefore, we performed a flecainide test in IV.2, who carries both the *SCN5A* and the loss-of-function *CACNA1C* mutation. Interestingly, infusion for 10 minutes with flecainide (also 2 mg/kg) in the patient IV.2 produced a QRS widening and a Brugada syndrome-like pattern, without modifying the QTc (Figure 7).

DISCUSSION

Here we functionally describe a novel missense mutation located at the distal C-terminal domain of Cav1.2 (p.S1961N). This mutation was found in a proband and 4 of his relatives belonging to a Spanish family with history of syncope and sudden cardiac death. The results demonstrated that the p.S1961N mutation decreased the I_{CaL} density, which probably shortens the duration of the plateau phase of the cardiac AP.

The oldest nephew of the proband had LQTS type 3 and was found to carry the p.R1644H Nav1.5 mutation. However, his mother, his brother, and his uncle (the proband) do carry the p.R1644H Nav1.5 mutation but did not show LQTS features. This could be explained by the frequent variable LQTS expressivity among carriers of a mutation, which, in some families can be

explained by the presence of multiple mutations in the same or different genes (compound or digenic heterozygosity, respectively) or by single nucleotide polymorphisms (SNPs).[9,10,21] Indeed, the functional compensation between mutations or polymorphisms within the *SCN5A* gene has been previously described.[10,22,23] Such is the case of the common Nav1.5 p.H558R polymorphism when it is presented in the same (*cis*) or in a different allele (*trans*) from the mutation.[10,21,23] Furthermore, it has been shown that 2 *SCN5A* mutations in *trans* (compound heterozygosity) can interact, ameliorating their deleterious effects reciprocally.[10,24] However, no additional polymorphisms or mutations were found in the *SCN5A* gene in any of the family members studied here.

Some *SCN5A* mutations can give rise to a wide spectrum of disease phenotypes among the different carriers, thus producing "overlapping syndromes".[11,25] In fact, the substitution of Arg by Cys at the same position (p.R1644C) of the Nav1.5 channels has been identified in families with either LQTS type 3[26] or Brugada syndrome.[27] However, this is not the case in our family, in which besides the LQTS type 3 phenotype of patient IV.1, no other electrocardiographic features suggesting other arrhythmic phenotype were identified. This is consistent with data previously reported regarding other families carrying the p.R1644H gain-of-function mutation, which has exclusively been associated with LQTS type 3.[17,18]

p.S1961N Cav1.2 Mutation Reduces L-type Ca Current Density

At physiologically relevant membrane potentials, the peak I_{CaL} density generated by p.S1961N Cav1.2 channels decreased by ~25% and the total charge crossing the membrane by ~40%. Conversely, when cells were simultaneously transfected with WT and p.S1961N Cav1.2 channels (0.5:0.5 ratio) to "reproduce" the heterozygous condition of the participants, the current decrease was lessened. These results agree with the mild-normal phenotype of the p.S1961N mutation carriers who exhibited normal ECG and QT intervals, either when they had it concurrently with the Nav1.5 mutation (III.1, III.2, IV.2) or when not (II.4 and III.4). Importantly, the hallmark of the mutation was the acceleration of the time course of Cav1.2 channel inactivation without any alteration of the voltage dependence of either activation or inactivation.

As mentioned, inactivation of Cav1.2 channels consists of CDI and VDI components.[19,28] CDI is mainly controlled by Ca/calmodulin binding to an IQ motif and is greatly inhibited when Ba is used as charge carrier.[19] Molecular determinants of VDI, which include, among others, the C-terminal domain of Cav1.2 channels, are multiple and complex.[28] Previous results demonstrated that mutations in the calcineurin (CaN)-binding site at the Cav1.2 channel (residues 1913-1941; NP_000710.5) markedly increase the VDI rate.[29] Furthermore, it was suggested that the CaN-binding site is the VDI regulatory motif of the Ca cardiac channel,[30] which partially overlaps with the protein phosphatase 2A (PP2A)-binding site (residues 1928-1970).[31] According to this, the p.S1961 residue lies in the C-terminal region of the PP2A-binding site. Our results demonstrated that the p.S1961N mutation mainly increases the VDI rate of Cav1.2 channels, and thus, it could be speculated that the mutation enhances the PP2A binding and/or function. Indeed, some studies have suggested that PP2A-mediated dephosphorylation of Cav1.2 channels inhibits their function by antagonizing the cAMP-dependent protein kinase-mediated I_{CaL} increase.[31] Finally, the novel loss-of-function mutation in *CACNA1C* gene that we have described might, by removing the serine at position 1961, eliminate a putative phosphorylation site. Indeed, this serine is predicted as a putative phosphorylation site for phosphoinositide-dependent kinase 1 (PDPK1) by bioinformatic predictions (Group-based prediction System 3.0), although it has not been demonstrated experimentally. Therefore, further studies are needed to determine the actual mechanism by which the mutation causes an acceleration of the VDI of Cav1.2 channels.

Clinical Implications of the Functional Findings in this Family

The results of the mathematical model confirmed that the I_{NaL} increase produced by the p.R1644H Nav1.5 mutation could be responsible for the prolongation of the APD and QT interval duration observed in IV.1. Conversely, the slight decrease in the Ca influx during the plateau phase of the human cardiac AP produced by the p.S1961N Cav1.2 mutation could compensate the increase in the Na influx produced by the p.R1644H Nav1.5 mutation. Consequently, those family members that harbour both mutations would exhibit "almost normal" ventricular APs and ECG. However, we must keep in mind that the proband, who carries both mutations, had a syncopal episode when he was under treatment with ciprofloxacin, an antibiotic that increases the QT interval.[15] Furthermore, both the mother and the grandmother of the proband, who seem to be "obligate carriers" of both mutations (the proband's father does not have any of the mutations), experienced sudden cardiac death. Of note, in patient IV.2, who also carries both mutations, flecainide infusion produced a noticeable QRS widening and a Brugada syndrome-like pattern, without any modification of the QT duration. Therefore, it can be hypothesized that the "functional compensation" between the gain-of-function and loss-of-function mutations of the Na and Ca channels, respectively, seems to be limited to conditions in which the genetic background of the patients does not concur with other factors that either prolong the ventricular repolarization (such as drugs, bradycardia, and electrolyte disturbances) or decrease cardiac excitability and/or shorten the duration of the plateau phase of the ventricular AP (such as flecainide). Therefore, it seems that in the patients carrying both mutations, either *torsades de pointes*- or Brugada syndrome-associated arrhythmias could be generated as a function of different proarrhythmic factors.

CONCLUSIONS

These results further support the contention that variable penetrance and phenotypic expressivity of arrhythmogenic inherited syndromes are partially attributable to genetic factors. In this context, functional analysis could help to select phenotype-based therapy in each family member.

ACKNOWLEDGEMENTS

We thank Sandra Sacristán, Lorena Ondo, and Paloma Vaquero for their invaluable technical assistance.

FUNDING

This work was supported by Fondos Europeos de Desarrollo Regional; Ministerio de Economía y Competitividad [SAF2014-58769-P; SAF2017-88116-P]; Comunidad Autónoma de Madrid [B2017/BMD-3738]; Instituto de Salud Carlos III [PI16/00398]; The ERA-Net for Research on Rare Diseases (AC14/00029), Mutua Madrileña and Banco Bilbao Vizcaya Argentaria Foundations, and the Spanish Society of Cardiology Grants.

CONFLICTS OF INTEREST

None declared.

WHAT IS KNOWN ABOUT THE TOPIC?

At least 15 genes have been linked so far to LQTS, an inherited primary arrhythmogenic syndrome characterized by a prolonged QT interval that increases the risk of sudden cardiac death due to ventricular fibrillation. LQTS shows marked phenotypic expressivity, which has been mainly attributed to demographic factors and greatly hampers risk stratification in patients and therapeutic decisions. However, in some families, the variable expressivity is due to genetic factors and can be explained by the presence of multiple mutations in the same or different genes (compound or digenic heterozygosity, respectively) or by SNPs.

WHAT DOES THIS STUDY ADD?

We functionally analyzed a mutation in the *CACNA1C* gene encoding p.S1691N Cav1.2 channels found in digenic heterozygosity in a Spanish family. The results demonstrated that this mutation decreased the Ca influx during the plateau phase of the AP, an effect that functionally counterbalances the increase in the Na influx produced by the long QT-associated *SCN5A* mutation encoding p.R1644H Nav1.5 channels. As a consequence, only the family member carrying the SCN5A mutation exclusively exhibits LQTS type 3. Therefore, phenotypic expression of LQTS could be modulated by genetic factors and the functional analysis of concurrent mutations could help to guide a personalized therapeutic approach.

SUPPLEMENTARY MATERIAL

Supplementary material associated with this article can be found in the online version available at https://doi.org/10.1016/j.rec.2014.04.021

REFERENCES

1. Nakano Y, Shimizu W. Genetics of long-QT syndrome. *J Hum Genet.* 2016;61:51–55.
2. Bohnen MS, Peng G, Robey SH, et al. Molecular pathophysiology of congenital Long QT Syndrome. *Physiol Rev.* 2017;97:89–134.
3. Savio-Galimberti E, Argenziano M, Antzelevitch C. Cardiac Arrhythmias Related to Sodium Channel Dysfunction. *Handb Exp Pharmacol.* 2017. http://dx.doi.org/10.1007/164_2017_43. Accessed 22 Feb 2018.
4. Rougier JS, Abriel H. Cardiac voltage-gated calcium channel macromolecular complexes. *Biochim Biophys Acta.* 2016;1863:1806–1812.
5. Burashnikov E, Pfeiffer R, Barajas-Martínez H, et al. Mutations in the cardiac L-type calcium channel associated with inherited J-wave syndromes and sudden cardiac death. *Heart Rhythm.* 2010;7:1872–1882.
6. Béziau DM, Barc J, O'Hara T, et al. Complex Brugada syndrome inheritance in a family harbouring compound SCN5A and CACNA1C mutations. *Basic Res Cardiol.* 2014;109:446.
7. Betzenhauser MJ, Pitt GS, Antzelevitch C. Calcium channel mutations in cardiac arrhythmia syndromes. *Curr Mol Pharmacol.* 2015;8:133–142.
8. Dumaine R, Wang Q, Keating MT, et al. Multiple mechanisms of Na^+ channel–linked long-QT syndrome. *Circ Res.* 1996;78:916–924.
9. Caballero R, Utrilla RG, Amorós I, et al. Tbx20 controls the expression of the KCNH2 gene and of hERG channels. *Proc Natl Acad Sci USA.* 2017;114:E416–E425.
10. Núñez L, Barana A, Amorós I, et al. p.D1690N Nav1.5 rescues p.G1748D mutation gating defects in a compound heterozygous Brugada syndrome patient. *Heart Rhythm.* 2013;10:264–272.
11. Dolz-Gaitón P, Núñez M, Núñez L, et al. Functional characterization of a novel frameshift mutation in the C-terminus of the Nav1.5 channel underlying a Brugada syndrome with variable expression in a Spanish family. *PLoS One.* 2013;8:1–15.
12. Richards S, Aziz N, Bale S, et al. Standards and guidelines for the interpretation of sequence variants: a joint consensus recommendation of the American College of Medical Genetics and Genomics and the Association for Molecular Pathology. *Genet Med.* 2015;17:405–424.
13. Matamoros M, Pérez-Hernández M, Guerrero-Serna G, et al. Nav1.5 N-terminal domain binding to α1-syntrophin increases membrane density of human Kir2.1, Kir2.2 and Nav1.5 channels. *Cardiovasc Res.* 2016;110:279–290.
14. O'Hara T, Virág L, Varró A, Rudy Y. Simulation of the undiseased human cardiac ventricular action potential: model formulation and experimental validation. *PLoS Comput Biol.* 2011;7:e1002061.
15. Tamargo J. Drug-induced torsade de pointes: from molecular biology to bedside. *Jpn J Pharmacol.* 2000;83:1–19.
16. Wang DW, Yazawa K, George AL, Bennett PB. Characterization of human cardiac Na^+ channel mutations in the congenital long QT syndrome. *Proc Natl Acad Sci USA.* 1996;93:13200–13205.
17. Splawski I, Shen J, Timothy KW, et al. Spectrum of mutations in long-QT syndrome genes. KVLQT1, HERG, SCN5A, KCNE1, and KCNE2. *Circulation.* 2000;102:1178–1185.
18. Kapa S, Tester DJ, Salisbury BA, et al. Genetic testing for long-QT syndrome: distinguishing pathogenic mutations from benign variants. *Circulation.* 2009;120:1752–1760.
19. Peterson BZ, DeMaria CD, Adelman JP, Yue DT. Calmodulin is the Ca^{2+} sensor for Ca-dependent inactivation of L-type calcium channels. *Neuron.* 1999;22:549–558.
20. Priori SG, Wilde AA, Horie M, et al. Executive summary: HRS/EHRA/APHRS expert consensus statement on the diagnosis and management of patients with inherited primary arrhythmia syndromes. *Heart Rhythm.* 2013;10:e85–e108.
21. Napolitano C, Novelli V, Francis MD, Priori SG. Genetic modulators of the phenotype in the long QT syndrome: state of the art and clinical impact. *Curr Opin Genet Dev.* 2015;33:17–24.
22. Poelzing S, Forleo C, Samodell M, et al. SCN5A polymorphism restores trafficking of a Brugada syndrome mutation on a separate gene. *Circulation.* 2006;114:368–376.
23. Viswanathan PC, Benson DW, Balser JR. A common SCN5A polymorphism modulates the biophysical effects of an SCN5A mutation. *J Clin Invest.* 2003;111:341–346.
24. Clatot J, Ziyadeh-Isleem A, Maugenre S, et al. Dominant-negative effect of SCN5A N-terminal mutations through the interaction of Na(v)1.5 α-subunits. *Cardiovasc Res.* 2012;96:53–63.
25. Remme CA, Wilde AA, Bezzina CR. Cardiac sodium channel overlap syndromes: different faces of SCN5A mutations. *Trends Cardiovasc Med.* 2008;18:78–87.
26. Napolitano C, Priori SG, Schwartz PJ, et al. Genetic testing in the long QT syndrome: development and validation of an efficient approach to genotyping in clinical practice. *JAMA.* 2005;294:2975–2980.
27. Frustaci A, Priori SG, Pieroni M, et al. Cardiac histological substrate in patients with clinical phenotype of Brugada syndrome. *Circulation.* 2005;112:3680–3687.
28. Hofmann F, Flockerzi V, Kahl S, Wegener JW. L-type Cav1.2 calcium channels: from in vitro findings to in vivo function. *Physiol Rev.* 2014;94:303–326.
29. Tandan S, Wang Y, Wang TT, et al. Physical and functional interaction between calcineurin and the cardiac L-type Ca^{2+} channel. *Circ Res.* 2009;105:51–60.
30. Cohen-Kutner M, Yahalom Y, Trus M, Atlas D. Calcineurin Controls Voltage-Dependent-Inactivation (VDI) of the Normal and Timothy Cardiac Channels. *Sci Rep.* 2012;2:366.
31. Hall DD, Feekes JA, Arachchige. et al. Binding of protein phosphatase 2A to the L-type calcium channel Cav1.2 next to Ser1928, its main PKA site, is critical for Ser1928 dephosphorylation. *Biochemistry.* 2006;45:3448–3459.